Available online at www.sciencedirect.com

ScienceDirect

Procedia CIRP 94 (2020) 21–24

www.elsevier.com/locate/procedia

11th CIRP Conference on Photonic Technologies [LANE 2020] on September 7-10, 2020

Laser powder bed fusion of WE43 in hydrogen-argon-gas atmosphere

Arvid Abel[a,*], Yvonne Wessarges[a], Stefan Julmi[b], Christian Hoff[a], Jörg Hermsdorf[a], Christian Klose[b], Hans Jürgen Maier[b], Stefan Kaierle[a], Ludger Overmeyer[a]

[a]*Laser Zentrum Hannover e.V., Hollerithallee 8, 30419 Hannover, Germany*
[b]*Institut für Werkstoffkunde, Leibniz Universität Hannover, An der Universität 2, 30823 Garbsen, Germany*

* Corresponding author. Tel.: +49-511-2788-482; fax: +49-511-2788-100. *E-mail address:* a.abel@lzh.de

Abstract

Growing demand for individual and especially complex parts with emphasis on biomedical or lightweight applications enhances the importance of laser powder bed fusion. Magnesium alloys offer both biocompatibility and low density, but feature a very high melting point of oxide layers while the evaporation temperature of pure magnesium is much lower. This impedes adequate part quality and process reproducibility. To weaken this oxide layer and enhance processability, a 2 %-hydrogen-argon-gas atmosphere was investigated. A machine system was modified to the use of the novel inert gas to determine the influence of gas atmosphere on hollow cuboids and solid cubes. While processing a 20.3 % decrease in structure width and 20.6 % reduction in standard deviation of the cuboids was determined. There was no significate influence on relative density of solid cubes although eight of the ten highest density specimen were fabricated with the hydrogen addition.

Keywords: additive manufacturing; laser powder bed fusion, magnesium, magnesium alloys, hydrogen

1. Introduction

The increasing demand for efficient transportation drives the research for lightweight materials especially in additive manufacturing. Furthermore, due to high human life expectancy, innovative solutions for individual and complex biomedical implants are under special focus of research. Magnesium as a material for laser powder bed fusion (also known as Powder Bed Fusion by Laser Beam, PBF-LB/M) suits both applications having a low density while being highly biocompatible [1]. First studies to fabricate single tracks out of magnesium were carried out by Ng et al. in 2009 [2]. They proved that the fabrication of sintered tracks is possible, despite the tendency of balling and spattering. Since then developments in magnesium alloy composition and processing parameters improved the processability [3,4]. The first dense specimen were created in 2012 using magnesium alloy AZ91 with a density of 99.5 %. However, the use of aluminum for alloying impairs the biocompatibility [4,5,6,7]. A promising magnesium alloy was created in 2016. With an yttrium (W) content of 4 % and rare earth elements (E) of 3 % this material (WE43) can be used as a biodegradable material. In PBF-LB a laser melts a multitude of particles in a powder bed, in which these particles are combined into geometric shapes. Due to the fabrication and handling of the magnesium powder, oxygen superficially oxidizes the particle's surface [8]. The obstacle in PBF-LB of magnesium is this formation of oxide layers. The challenge is the high melting point (2852 °C) of the enveloping oxide layer with respect to the pure magnesium's low vaporizing temperature (1110 °C). Due to this gap in processable temperature, the melt pools tend to overheat during the laser exposure. This leads to partial evaporations of the magnesium, which causes porosity [5]. This paper describes the use of a novel inert gas mixture and the effects on the processability of the magnesium alloy WE43 based on a series of investigations on hollow cuboids and solid cubes.

10.1016/j.procir.2020.09.005

2. Materials and methods

2.1. Machine set up and materials

The machine setup is a SLM125HL PBF-LB system by SLM Solutions GmbH (Luebeck, Germany) with a 100 W continuous wave ytterbium fiber laser. The laser has a focus diameter of 70 µm and a wavelength of 1070 nm. Carpenter Additive (Cheshire, Great Britain) supplied the WE43 alloy.

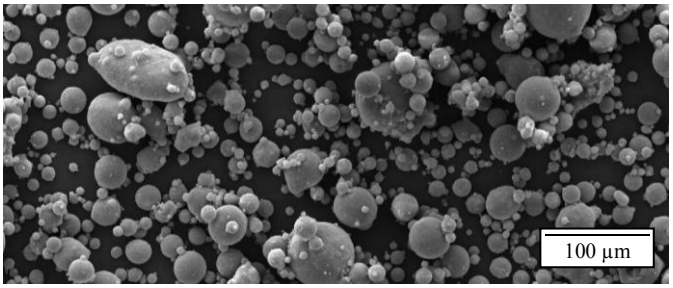

Fig. 1. WE43 powder

After the building process, the specimen are embedded in a two-component epoxy resin. Cross sections of the specimen will be made with a Tegramin-30 by Stuers (Ballerup, Denmark). The evaluation is based on microscopic images of these sections made with a Stemi 2000-C by Zeiss (Oberkochen, Germany) and a VK-X1000 by Keyence (Neu-Isenburg, Germany). The determination of width and density of these images is done with python scripts. To prevent negative consequences of hydrogen use, silica bags are applied in the process chamber, to absorb the resulting moisture of the reaction of hydrogen and the remaining oxygen, which impairs the flowability of the powder and thus the powder application.

2.2. Experimental set up and methods

In this paper, the influence of an admixture of hydrogen in the existing argon inert gas is investigated. This addition is set at 2 % to reduce the risk of oxyhydrogen detonating reactions, but to allow the remaining oxygen to be reduced to moisture, thus reducing oxidation of the molten magnesium. At first, investigations are carried out to determine the influence of the atmosphere on the structure width of single tracks in hollow cuboids. In a second step, the influence on solid cubes and their relative density is examined. The specimen are even cuboids with the dimension of 5 x 5 x 5 mm. The single track cuboids are directly connected to the build plate and the solid cubes are connected with a 1 mm line support structure.

The first series of investigations regarding the single tracks is divided into four blocks, depending on the atmospheric conditions as shown in table 1.

Table 1. Atmospheric conditions of the single track experiment.

Block	Inert gas	Build plate temperature in °C
I	100 % Argon	40
II	100 % Argon	200
III	98 % Argon; 2 % Hydrogen	40
IV	98 % Argon; 2 % Hydrogen	200

Each block is divided into four different laser exposure strategies, resulting in 16 groups:

- outer contour line
- an inner contour line
- a double outer laser line exposure
- outer and inner contour line

Within these groups, hollow cuboids with six different parameter sets are produced (Table 2). This results in a total number of 96 samples in the first study. The parameters are given by the statistic software JMP and originate from a preliminary test, with the aim to have a lower (20 W) und upper (100W) energy density boundary.

The expected result of these parameters is a non-melting of the powder at low power and a much wider melting than the laser spot diameter at high power. To get more statistical significance, the parameter with a medium energy density is fabricated twice. The ideal result of the melting process is a dense rectangular wall with the width of the laser spot. The adhesion of one particle layer is expected and so results up to 150 µm are targeted. Results above a wall thickness of 196 µm (i.e. adhesion of the largest particle diameter of 63 µm on both sides of the 70 µm spot) are not desired in this experiment, as an ideal thin structure is to be produced first.

Table 2. Laser parameters of the cuboids.

Number	Laser power in W	Scanning speed in $\frac{mm}{s}$
I	20	100
II	20	900
III	60	500
IV	60	500
V	100	100
VI	100	900

The second series of investigations regards the relative density of solid cubes with identical atmospheres according to the blocks in table 1. It considers two hatching strategies:

- chess pattern
- line pattern

Table 3 shows the investigated laser parameters. There is a full factorial experiment within a narrow interval. The hatch distance is set to 45 µm. The resulting total amount of the investigated cubes is 72.

Table 3. Laser parameters for the cubes.

Number	Laser power in W	Scanning speed in $\frac{mm}{s}$
I	75	400
II	80	400
III	85	400
IV	75	450
V	80	450
VI	85	450
VII	75	500
VIII	80	500
IX	85	500

3. Experimental Results

3.1. Results of the first investigation

The results of the first investigation show the influence of laser parameters, different hatching strategies and atmospheric condition. The figure 2 shows an exemplary build plate with unextracted specimen and the table 4 shows the overall results, differentiated by laser parameter, forming averages over all atmospheric conditions and exposure strategies. Figure 2 illustrates the evaluation. Three specimens with good and two with undesirable structures can be identified. One of these specimens has too thin and the other too thick structures.

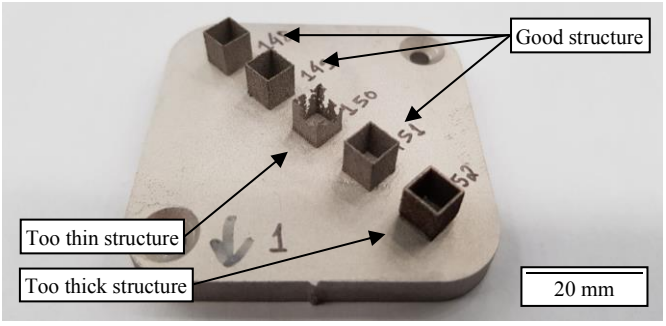

Fig. 2. Single track specimen

Figure 3 shows cross sections of wall structures. The one on the left is too thin, is middle is desirable and the one on the right is too thick. The ideal wall thickness is between 100 to 140 µm, forming a solid wall with the thickness of the laser spot (70 µm) with some adhering particles.

Fig. 3. Cross sections of different wall structures, left too thin (65.2 µm), middle desirable (115.2 µm), right too thick (203.1 µm)

The evaluation is shown in the table 4. Only the parameter III and IV (which are the same) resulting in a thin consistent structure. Thus, 32 desirable test specimens were selected in order to evaluate the influence of the exposure strategy and the atmospheric conditions in the next steps.

Table 4. Averaged results of the cuboids, differentiated by laser parameter

No.	Mean width in µm	Mean standard deviation in µm	Evaluation of the structure
I	84.8	38.7	Too thin & inconsistent
II	-	-	Powder did not melt
III	137.4	24.4	Thin & consistent
IV	140.8	27.0	Thin & consistent
V	590.1	16.8	Too thick & consistent
VI	158.0	33.8	Thin & slightly inconsistent

Table 5 shows the averaged results of the 32 most desirable selected cuboids in structure width and standard deviation differentiated by exposure strategy, averaging the atmospheric conditions. It is displayed that the exposure strategy has no influence on the mean width or the standard deviation.

Table 5. Averaged results of the best cuboids, differentiated by exposure strategy

Exposure strategy	Mean width in µm	Standard deviation in µm
Outer contour	138.7	25.0
Outer contour double	139.0	25.6
Inner contour	139.5	26.9
Double contour	139.3	25.5

The mean values of the wall thickness of the selected cuboids, differentiated by atmospheric conditions are shown in table 6. It is displayed, that the addition of hydrogen in the inert gas decreased the width by 20.3 % and the standard deviation by 20.6 %. There is an influence of the build plate temperature, but it is not systematic.

Table 6. Averaged results of the best cuboids, differentiated by atmospheric condition

Block	Mean width in µm	Standard deviation in µm
I (Ar – 40 °C)	148.9	27.9
II (Ar – 200 °C)	160.8	29.5
III (H_2 – 40 °C)	119.7	23.3
IV (H_2 – 200 °C)	127.2	22.3

3.2. Results of the second investigation

The following results display the influence of the build plate preheating temperature, the hatching strategy and the hydrogen addition in the inert gas on the relative density on solid cubes. Figure 4 displays the analyzed cross sections as examples with two different relative densities. These cubes were fabricated with identical parameters except for scanning speed.

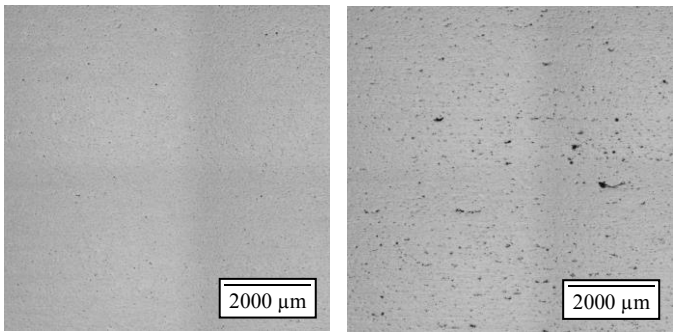

Fig. 4. Cross sections of cubes (H_2, 200 °C, 75 W and 45 µm chess hatching). Left 99.86 % (400 mm/s) and right 98,99 % (450mm/s) relative density

Table 7 shows the mean relative densities of the cubes differentiated by build plate preheating. The difference in median is below the standard deviation, thus negligibly small.

Table 7. Averaged results of the cubes, differentiated by heating temperature

Parameter	Rel. density at 40 °C in %	Rel. density at 200 °C in %
I	99.84	99.91
II	99.70	99.85
III	99.53	99.76
IV	99.57	99.64
V	99.91	99.88
VI	99.65	99.80
VII	99.52	99.35
VIII	99.61	99.60
IX	99.75	99.65
Median	99.67	99.72
Std. deviation	0.13	0.17

The influence of the hatching strategy is displayed in table 8. The mean values over all samples show a difference in 0.25 % density and the standard deviation is reduced by a factor of 4.

Table 8. Averaged results of the cubes, differentiated by hatching strategy

Parameter	Rel. density with chess hatching in %	Rel. density with line hatching in %
I	99.86	99.88
II	99.67	99.88
III	99.51	99.78
IV	99.42	99.79
V	99.89	99.91
VI	99.63	99.83
VII	99.04	99.84
VIII	99.49	99.73
IX	99.61	99.75
Median	99.57	99.82
Std. deviation	0.24	0.06

The table 9 shows the results differentiated by inert gas. It is shown that the difference in density is below the standard deviation and therefore the hydrogen shows no significate influence on mean value. However, eight of the ten specimen with the highest density are fabricated with hydrogen.

Table 9. Averaged results of the cubes, differentiated by inert gas

Parameter	Rel. density Ar in %	Rel. density H_2 in %
I	99.86	99.89
II	99.74	99.82
III	99.57	99.73
IV	99.63	99.58
V	99.85	99.94
VI	99.70	99.75
VII	99.44	99.43
VIII	99.62	99.60
IX	99.69	99.69
Median	99.68	99.71
Std. deviation	0.12	0.15

4. Conclusion

This investigation shows the influence of a 2 % hydrogen addition in a pure argon inert gas on the production of hollow cuboids and solid cubes in the PBF-LB with the magnesium alloy WE43. The first investigation determined the influence of the inert gas on single track structures in hollow cuboids. Different laser exposure strategies were applied but no impact occurred. A decrease of 20.3 % in structure width and a 20.6 % decrease in the associated standard deviation was shown, due to the addition of hydrogen in the inert gas. Which is a significate improvement and shows the potential of the research in atmospheric parameters in the PBF-LB process.

The second investigation carried out a series of experiments to determine the influence of the inert gas on the relative density of solid cubes. The admixture of hydrogen and the build plate preheating showed no significate influence in terms of mean values of the density. Nevertheless, eight out of the best ten results were fabricated with hydrogen and five of these eight were fabricated with 200 °C plate temperature. It is shown that the line hatching improves the density and significantly reduces the standard deviation. It is suspected that there will be a noticeable difference in a wider process parameter interval, due to the major improvements in the first investigation.

The next steps will be a series of investigations to determine if the hydrogen addition causes a shift of optimal process parameters of the relative density. This should improve the robustness of the process and increase the volume generation rate. The influence on surface roughness of the generated geometries, the microstructure of the building specimen and the tensile properties should be determined.

Acknowledgements

The authors gratefully acknowledge the funding by the German Research Foundation (DFG) within the priority program (SPP) 2122 “Materials for Additive Manufacturing (MATframe)”.

References

[1] Manakari et al., V., Selective Laser Melting of Magnesium and Magnesium Alloy Powders: A Review, Department of Mechanical Engineering, Nation University of Singapore, Journal Metals, 2017.
[2] Ng et al., C.C., Selective Laser Melting of Magnesium Alloys, Rapid Prototyping Journal, Vol. 17, 2011.
[3] Gieseke et al., M., Selective Laser Melting of Magnesium and Magnesium Alloys, Rapid Tech 2015, Erfurt, Trade forum “Science”, 2015.
[4] Wessarges et al., Y, Selective Laser Melting of Magnesium Alloys for Biomedical Applications, Proceedings of 6th International Conference on Additive Manufacturing, Nürnberg, 2016.
[5] Jauer et al., L., Selective Laser Melting of Magnesium Alloys, Fraunhofer Institut for Laser Technology ILT, AKL2016, Aachen, 2016.
[6] Gieseke et al., M., Selective Laser Melting of Magnesium Alloys for Manufacturing Individual Implants, DDMC 2014 Fraunhofer Direct Digital Manfacturing Conference, Berlin, 2014.
[7] Tandon et al., R., Emerging applications using magnesium alloy powders: A feasibility study, Magnesium Technology 2014, The Minerals, Metals & Materials Society, 2014.
[8] Gieseke et al., M., Challenges of processing Magnesium and Magnesium Alloys by Selective Laser Melting, World PM2016, Procedings, 2016